HHS Public Access

Author manuscript

Geoderma. Author manuscript; available in PMC 2023 November 03.

Published in final edited form as:

Geoderma. 2023 April ; 432: . doi:10.1016/j.geoderma.2023.116377.

Mechanisms and health implications of toxicity increment from arsenate-containing iron minerals through *in vitro* gastrointestinal digestion

Ruiqi Liu[a], **Shuqiong Kong**[a,*], **Yixian Shao**[b], **Dawei Cai**[a], **Bing Bai**[a], **Xiaguo Wei**[a], **Robert A. Root**[c], **Xubo Gao**[a], **Chengcheng Li**[d], **Jon Chorover**[c]

[a]School of Environmental Studies, China University of Geosciences, Wuhan 430074, Hubei, PR China

[b]Zhejiang Institute of Geological Survey, Hangzhou 311203, Zhejiang, PR China

[c]Department of Environmental Science, University of Arizona, Tucson, AZ 85721, United States

[d]State Key of Biogeology and Environmental Geology Laboratory, China University of Geosciences, Wuhan 430074, Hubei, PR China

Abstract

Inadvertent oral ingestion is an important exposure pathway of arsenic (As) containing soil and dust. Previous researches evidenced health risk of bioaccessible As from soil and dust, but it is unclear about As mobilization mechanisms in health implications from As exposure. In this study, we investigated As release behaviors and the solid–liquid interface reactions toward As(V)-containing iron minerals in simulated gastrointestinal bio-fluids. The maximum As release amount was 0.57 mg/L from As-containing goethite and 0.82 mg/L from As-containing hematite at 9 h, and the As bioaccessibility was 10.8% and 21.6%, respectively. The higher exposure risk from hematite-sorbed As in gastrointestinal fluid was found even though goethite initially contained more arsenate than hematite. Mechanism analysis revealed that As release was mainly coupled with acid dissolution and reductive dissolution of iron minerals. Proteases enhanced As mobilization and thus increased As bioaccessibility. The As(V) released and simultaneously transformed to high toxic As(III) by gastric pepsin, while As(V) reduction in intestine was triggered by pancreatin and freshly formed Fe(II) in gastric digests. $CaCl_2$ reduced As bioaccessibility, indicating that calcium-rich food or drugs may be effective dietary strategies to reduce As toxicity. The results deepened our understanding of the As release mechanisms associated with iron minerals in the simulated gastrointestinal tract and supplied a dietary strategy to alleviate the health risk of incidental As intake.

*Corresponding author at: School of Environmental Studies, China University of Geosciences, Wuhan, 388 Lumo Road, Hongshan District, Wuhan 430074, Hubei, PR China. ksq@cug.edu.cn (S. Kong).

Declaration of Competing Interest

The authors declare that they have no known competing financial interests or personal relationships that could have appeared to influence the work reported in this paper.

Appendix A. Supplementary data

Supplementary data to this article can be found online at https://doi.org/10.1016/j.geoderma.2023.116377.

Keywords

Bioaccessibility; As release; Dissolution; Arsenate-containing iron minerals

1. Introduction

Arsenic (As) is a toxic metalloid that is extremely harmful to mammals and widely distributed in the natural environment. Both natural geological processes and anthropogenic activities cause As accumulation in surficial ecosystems where it can lead to contamination of water and soil, and ultimately endangers human health (Rahaman et al., 2021). Incidental oral ingestion is considered an important exposure pathway for As-containing soil and dust, such as agricultural activities of As-contaminated area, residents neighboring mines and children through frequent hand-to-mouth behaviors (Lin et al., 2017). Chronic exposure to soil As is associated with a variety of adverse health effects, including cancers and neurological and cardiovascular effects (Wang et al., 2018). Approaches to assess health risks of As usually include *in vivo* animal models and *in vitro* simulations. *In vivo* models are relatively close to reality, but they are also technically difficult, costly, poorly reproducible and limited by ethical constraints (Guerra et al., 2012). *In vitro* methods are convenient, rational and replicable, therefore, they are increasingly used as alternatives to *in vivo* studies (Juhasz et al., 2014). The most extensive *in vitro* bioaccessibility (IVBA) studies are based on biochemical parameters that mimic the physicochemical and enzymatic process (Thomas et al., 2018). Many factors lead to the variability in As bioaccessibility in As-contaminated soil or dust, including As source and speciation, soil particle sizes and mineralogical composition (Yin et al., 2021; Yin et al., 2022). Bioaccessibility is defined as the fraction of As that is soluble in the *in vitro* bio-fluid and available for absorption (Yin et al., 2020). Arsenic bioaccessibility is positively correlated with As release amount from solid matrix when the total As content in solid matrix is constant. The *in vitro* gastrointestinal (IVG) assay is a validated bioaccessibility model, it offers unique advantages of good repeatability and high correlation with *in vivo* As bioavailability model (Juhasz et al., 2014).

Arsenic bioaccessibility depends on reaction conditions, such as As concentration and speciation, and gastrointestinal bio-fluids physicochemical parameters. Arsenate ($As^{V}O_4^{3-}$) is the dominant As speciation in topsoil and dust, and it tends to be chemically or microbially reduced to arsenite ($As^{III}O_3^{3-}$) in the human gastrointestinal tract (Van de Wiele et al., 2010). It is paramount to assess the proportion of As(III) in gastrointestinal tract since the toxicity of As(III) has been shown to be circa 60 times greater than As(V) (Cai et al., 2022b; Rahaman et al., 2021). Previous work show that As bioaccessibility in As-containing goethite is 52.6 – 74.6% in colon digest, and that the proportions of dissolved As(III) is 59.5 – 76.7% (Yin et al., 2020). The fraction of As(III) in the bioaccessible As release from soil is up to 71% in anaerobic gastrointestinal environment (Li et al., 2021). Furthermore, As bioaccessibility can be affected by physicochemical properties of digestive tract due to the high complexity and dynamicity of gastrointestinal environment. Previous work reported that pH and digestive enzymes strongly impact As speciation and mobility (Smith et al., 2014). As(III) and As(V) dissolved in the gastric phase are removed from solution by

co-flocculation with ferric ion in intestinal phase due to the drastic increase of pH (Yu et al., 2016). Enzymes are dissolved organic matter (DOM) that can bind As(V) or As(III) and Fe(III) to form As-Fe-OM ternary complexes by ligand exchange and promote As release (Xiao et al., 2021). Besides, enzymes served as an effective protective layer to inhibit metals dissolution because of the physical barrier effect (Zhang et al., 2022). Coexisting ions and common food matrices also affect As bioaccessibility and speciation, glutathione cysteine and grape extract reduced the As solubility, vitamin and protein increased the As solubility and methylation percentages (Clemente et al., 2016; Wang et al., 2018; Yang et al., 2022).

Iron (hydr)oxides are widely existed in soil and dust, with large specific surface area, variable electrostatic charge and high activity, controlling the migration and transformation of As (Hammond et al., 2020). The reactive hydroxyl groups of iron (hydr)oxides have pH dependent charge by proton dissociation or association, representing the prevalent sources of positive surface charge in soil and dust (Schwertmann and Cornell, 2000). Arsenic mainly exists as oxygen anion in neutral environment (Song et al., 2015). As(III) and As(V) species adsorb to the iron (hydr)oxides via electrostatic attraction and ligand exchange reactions, resulting in adsorptive retention (Barron et al., 2022). Generally, As(V) reduction to As(III) leads to As release from As-containing iron minerals since the adsorptive retention of As(V) is stronger than that of As(III) (Dixit and Hering, 2003). Reductive dissolution of As-containing Fe(III)-(oxyhydr)oxides results in Fe(III) in lattice reduction to Fe(II) and release in neutral to acidic environments, thereby increasing As mobilization (Cai et al., 2020a). Hematite (Fe_2O_3) and goethite (α-FeOOH) are ubiquitous crystalline iron oxides in soil and dust, they are typical representative iron minerals and act as important specific adsorbents for As. The percentage of goethite was 10% and hematite was 2% in As contaminated soil (Meunier et al., 2010). Arsenic was predominantly formed inner-sphere monodentate complexes on the surface of goethite and formed outer-sphere complexes on hematite, and the affinity toward As was different between goethite and hematite (Brechbühl et al., 2012). Therefore, an in-depth understanding of goethite/hematite-associated As bioaccessibility is key to elaborate As biogeochemistry behavior of As-containing iron minerals in soil and dust (Schwertmann and Cornell, 2000). Most *in vitro* studies focus on distribution and health risk evaluation of As-containing soil and dust (Wang et al., 2021). However, As release and species transformation pathways are not clear during *in vitro* gastrointestinal digestion due to the complexity of bio-fluid assay. In addition, the knowledge gap remains in toxicity change of As-containing iron minerals ingested by human being.

The current work seeks to address this gap. The objectives of this work were to: 1) elucidate the As speciation transformation mechanisms using goethite and hematite as model iron minerals in soil and dust; 2) unveil the relationship of As liberation and digestion biogeochemistry behavior; 3) provide a feasible dietary strategy to alleviate As bioaccessibility in chronically exposed populations. The findings help to better understand the arsenic mobility and toxicity associated with iron minerals and predict health implication of arsenic exposure in human gastrointestinal tract accurately.

2. Materials and methods

2.1. Preparation of As(V)-containing goethite and hematite

Goethite (α-$Fe^{(III)}OOH$) and hematite ($FE_2^{(III)}O_3$) were synthesized according to Schwertmann and Cornell (2000). Detailed process is described in Text S1 of the Supporting Information (SI). The synthesized minerals were identified as goethite and hematite with good crystallization and high purity by X-ray diffraction (Figure S1). The specific surface area of goethite and hematite measured by the BET method was 57.56 and 39.24 $m^2.g^{-1}$, respectively.

According to mineral adsorption capacity and practical As contamination scenario, our adsorption experimental conditions were set as 0.01 g iron minerals with 1 mg/L or 5 mg/L arsenate solution at pH 7.0. The ratio of solid to solution was 0.01 g solid to 10 mL of As(V) solution in 50 mL polypropylene centrifuge tubes that were equilibrated at 200 rpm under 37°C for 72 h. Specifically, equilibrium As(V) adsorption onto goethite and hematite was 1.1 and 0.9 mg/g for 1 mg/L arsenate solution, denoted as G_L and H_L. The equilibrium As(V) adsorption onto goethite and hematite was 5.3 and 3.8 mg/g for 5 mg/L arsenate solution, denoted as G_H and H_H (Figure S2). All arsenate concentrations were relevant to the actual contamination environment, especially soil and dust affected by mining or agricultural activities (Meunier et al., 2010).

2.2. In vitro gastrointestinal simulation

A modified IVG method was used as a human gastrointestinal simulator, which consisted of two consecutive steps to simulate gastric and intestinal digestion stages (Juhasz et al., 2014). Gastrointestinal digestive enzymes including pepsin (Porcine, catalogue No. P-7000), pancreatin (Porcine, catalogue No. P-1750) and bile salt (Porcine, catalogue No. B-8631) were purchased from Sigma Chemical Co. (St. Louis, MO, USA). The detailed information about the IVG method is as follows:

Gastric phase: acid solution of 10 g/L porcine pepsin and 0.01 M NaCl, with pH adjusted to 1.5 using 2 M HCl. The digests headspace was flushed with $N_2(g)$ for 3 min to deoxygenate and shaken the centrifuge tubes under 200 rpm, 37°C for 1 h. The centrifuge tubes were wrapped with aluminum foil to avoid the interference from light.

Intestinal phase: the acidic chyme sample from gastric bio-fluid was adjusted to pH 6.5 with 1 M $NaHCO_3$ solution, followed by the addition of 36 mg bile salt (3.6 g/L) and 3.6 mg porcine pancreatin (0.36 g/L). Headspace was flushed with $N_2(g)$ for 3 min immediately and shaken the centrifuge tubes under 200 rpm, 37°C for an additional 8 h. Supernatants were filtered through 0.45 μm nylon membrane anoxically in the glovebox and stored at 4°C until analysis. All experiments were performed in triplicate.

2.3. Influence of digestion biochemistry on arsenic release

We investigated the effects of acid and pepsin (in gastric bio-fluid) as well as HCO_3^-, bile salt, pancreatin (in intestinal bio-fluid) on As release and transformation. In brief, the simulated gastric bio-fluid experiments included control groups in the absence of pepsin (pH 1.5) and

experimental groups (10 g/L pepsin, pH 1.5). The simulated intestinal bio-fluid experiments included bile salt (3.6 g/L bile salt, pH 6.5), pancreatin (0.36 g/L pancreatin, pH 6.5), mixed bile salt and pancreatin (3.6 g/L bile salt, 0.36 g/L pancreatin, pH 6.5), and control groups (pH 6.5). All digestive enzymes concentrations were based on the IVG model. Additionally, we compared the absence or presence of gastric digests before intestinal phase to investigate the effect of gastric chyme on As release and speciation in intestinal phase. The influence of typical nutrients (sucrose, starch, cellulose, oleic acid, glutathione and $CaCl_2$) on As release was determined to provide possible dietary approaches to reduce As bioaccessibility. Nutrient additions were based on reference intake for Chinese people (Table S1) (Tian and Yu, 2013).

2.4. Aqueous phase analysis

Samples for aqueous phase analysis were filtered through 0.45 μm nylon membranes. Dissolved Fe(II) and total Fe were quantified by 1,10-phenanthroline method at 510 nm with a U3900 spectrophotometer (UV–vis, U3900, Hitachi, Japan) (Hong et al., 2018). Arsenic speciation analysis was conducted using hydride generation-atomic fluorescence spectrometry (Titan Instrument Co. ltd., Beijing, P. R. China) (Hong et al., 2018). Detailed process is described in S1 (Text S2). The pH of gastrointestinal bio-fluids was measured by a pH meter (PHS-3E, Lichen, P. R. China). Correlation analysis between concentrations of dissolved Fe(II) and As(III) was conducted using IBM SPSS 25.0 software. One-way analysis of variance (ANOVA) followed by Dunnett's Test was performed to determine the significant difference in bioaccessible As concentrations among the six dietary component batches. Differences were considered significant for $p < 0.05$.

2.5. Solid phase characterization

Goethite and hematite with high As content were selected for solid phase characterization. Mineralogical changes after As adsorption and IVG reaction were examined by X-ray diffraction (XRD, Bruker AXS D8 Advance, Germany). Diffractograms were collected using a DX2700 diffractometer with a Cu-Kα X-ray source (40 kV, 40 mA), radiation in step scan mode between 15° and 75° 2θ with 0.01° step with a scanning speed of 10° min^{-1}. The surface area of unreacted goethite and hematite were determined using Brunauer-Emmett-Teller (BET) method after degassing under N_2 stream at 120°C for 6 h (BET, Micromeritics ASAP 2460, P. R. China). Molecular structure and chemical bond changes were analyzed using attenuated total reflectance fourier transform infrared spectrometer (ATR-FTIR, Nicolet iS50, ThermoFisher Scientific, USA), with scans across the wavenumber range of 650 – 4000 cm^{-1} at 4 cm^{-1} resolution. Surface elemental analysis was investigated with X-ray photoelectron spectrometer (XPS, K-Alpha, ThermoFisher Scientific, Escalab 250XI, USA) using a monochromatic Al Kα X-ray source. Data processing for XPS and XRD used Avantage 5.9921 and Jade 6.5.

3. Results and discussion

3.1. Release of arsenic and iron in simulated bio-fluids

The amount of As release followed the trend $H_H > G_H > H_L > G_L$ in simulated gastric and intestinal bio-fluid, whereas Fe release followed the trends $H_L > H_H > G_H > G_L$ in

gastric bio-fluid and $H_L > H_H > G_L > G_H$ in intestinal bio-fluid (Table 1). In the simulated gastric bio-fluid, the As release was 0.09 to 0.26 mg/L for goethite and 0.12 to 0.29 mg/L for hematite. Similarly, the dissolved Fe was 4.40 to 4.95 mg/L for hematite, while lower Fe values from 2.25 to 2.84 mg/L were observed for goethite. The total amounts of As and Fe release were linearly correlated in simulated gastric (R^2 = 0.87) and intestinal (R^2 = 0.90) bio-fluids. Dissolution of iron minerals apparently promoted As release, especially for hematite.

The maximum As release was 0.53 mg/L from H_H and 0.31 mg/L from G_H in intestinal bio-fluid; and lower As release from H_L and G_L was found, 0.07 and 0.05 mg/L, respectively (Table 1). Arsenic released from high As-containing iron minerals to gastric bio-fluid, then continuously released into intestinal bio-fluid. Whereas more As released into gastric rather than intestinal bio-fluid from low As-containing iron minerals, due to the limited initial As loading. Besides, As release behavior was also related to the dissolution and precipitation of iron minerals. The release of iron in the simulated intestinal bio-fluid was less than 24% in the simulated gastric bio-fluid, since the higher intestinal pH at 6.5 probably promoted re-precipitation of dissolved iron (Thomas et al., 2018). There was no sharp decrease in As release amount from simulated gastric to intestinal bio-fluid, though Fe precipitated in the intestinal bio-fluid. Some proteinases and coexisting ions in the simulated intestinal bio-fluid may have high complexation capacity to compete with iron minerals surface for As sorption, leading to As release into the intestinal bio-fluid (Yan et al., 2022).

3.2. Speciation of arsenic and iron in simulated bio-fluids

Dissolved As(III) concentrations ranged from 0.04 mg/L (I-G_L) to 0.24 mg/L (S-H_H), being 73.4% to 83.8% of total As at the end of gastric or intestinal digestion (Fig. 1a and Table S2). This highlighted As toxicity increment from As-containing iron minerals during *in vitro* gastrointestinal digestion, for the reason that arsenite is much more toxic and mobile than arsenate (Cai et al., 2022b; Rahaman et al., 2021). The maximum cumulative release of total As from goethite and hematite was 0.57 and 0.82 mg/L, and the As bioaccessibility was 10.8% and 21.6% in the gastrointestinal assay, respectively (Fig. 1a and 1b). Arsenic adsorption on goethite was 120 – 140% greater than hematite (Figure S2), while As release from As-containing goethite was 50 – 90% less than hematite. This indicated that there was a greater health risk for As-containing hematite than goethite. The phenomenon attributed to the differences of arsenic complexed with iron minerals due to the different surface area and crystalline structure between goethite and hematite. A shorter As-Fe distance was observed in As-containing goethite than in hematite, indicating that arsenic was more tightly bound to goethite and therefore less arsenic was released (Zhu et al., 2019). Previous work indicate that mineral composition of soil and dust affect As bioaccessibility (Meunier et al., 2010). Additionally, due to high affinity for arsenate sorption, increasing poorly crystalline ferric (hydr)oxides decreased As release (Thomas et al., 2018).

The bioaccessible As(III) was highly variable among various enzymes conditions in gastric bio-fluids. A large amount of bioaccessible arsenite was detected in the presence of pepsin, 0.11 mg/L from S-G_H and 0.24 mg/L from S-H_H, whereas the bioaccessible As(III) was below detection limit in the absence of pepsin (Table 2). This showed that pepsin acted

as an electron donor in simulated gastric bio-fluid, reducing As(V) to As (III). Following the gastric digestion, we added an intestinal phase without gastric digests to assess the reducibility of gastric chyme as well as bile salt, pancreatin in intestinal bio-fluid. Arsenite was not detected when intestinal fluid contained only bile salts, whereas obvious arsenite was measured after the addition of pancreatin, being 0.12 mg/L from I-G_H and 0.14 mg/L from I-H_H (Table 2). Accordingly, pancreatin acted as an electron donor, leading to arsenate reduction in simulated intestinal bio-fluid. Furthermore, the released arsenite was 0.14 mg/L from I-G_H and 0.23 mg/L from I-H_H in the intestine with gastric digest (Fig. 1a), higher than in the intestine without gastric digest, 0.12 mg/L from I-G_H and 0.14 mg/L from I-H_H (Table 2). Therefore, Fe(II) generated in gastric chyme contributed to arsenate reduction besides pancreatin in intestinal bio-fluid, and the reducing ability of pancreatin to As(V) was more prominent than that of Fe(II). Besides, tyrosine is one of the basic components of pepsin and pancreatin, and phenolic substances in its structure reduce ferric iron to ferrous iron, also confirming that the reductive ability of pepsin and pancreatin is stronger than that of Fe(II) (Wan et al., 2018).

The Fe(II) release amount ranged from 2.12 – 3.04 mg/L in simulated gastric bio-fluid, accounting for 61.5 – 94.2% of total Fe release in this step. Fe(II) amounted to 0.11 – 0.49 mg/L in intestinal bio-fluid, accounting for 61.6 – 83.0% of total Fe release in the second step (Fig. 1c and Table S2). The dissolution mechanisms of iron minerals included acidic dissolution and reductive dissolution, the former dissolved in the form of Fe(III), and the latter dissolved in the form of Fe(II) (Menacherry et al., 2018). Importantly, released Fe(II) was 2.67 mg/L from S-G_H and 2.85 mg/L from S-H_H in the presence of pepsin, respectively, whereas Fe(II) was not detected in the absence of pepsin (Table 2). There was no significant effect of pepsin on total iron release behavior. The results showed that Fe(III) mainly released from iron minerals into simulated gastric bio-fluid through acidic dissolution, and then gradually reduced to Fe(II) by free pepsin. Besides pepsin, the freshly formed Fe(II) also reduced As(V) to As(III), but its reducing ability to As(V) was weaker than pepsin, for reductant had higher reduction capacity than reduced product. The total Fe*(aq)* concentration was below detection limit for goethite (I-G_H) in the intestinal phase without gastric digest, and for hematite (I-H_H), total Fe*(aq)* concentration was 0.22 mg/L (Table 2). All the Fe*(aq)* concentrations were lower than those in intestinal phase that included the earlier gastric digest, being 0.67 mg/L for I-H_H and 0.13 mg/L for I-G_H (Table 1). Consequently, we deduced that the inclusion of gastric phase made the residual solid phase iron more susceptible to dissolution in the intestinal phase. Electron transfer between Fe(II) produced in gastric bio-fluid and Fe(III) oxides was invoked to explain Fe(II)-catalyzed reductive dissolution in intestinal bio-fluid (Notini et al., 2018). Besides, pancreatin inhibited iron dissolution and reduction. The values of total Fe and Fe(II) for bile group were 0.56 and 0.44 mg/L from I-H_H, higher than the mixed bile and pancreatin group, being 0.22 mg/L total Fe and 0.16 mg/L Fe(II). This was owing to the physical barrier effect of pancreatin by chelating, binding and adsorbing on the iron minerals surface (Zhang et al., 2022).

3.3. Relationship of arsenic and iron speciation in simulated bio-fluid

Fe(III) and As(V) were reduced to Fe(II) and As(III) simultaneously during simulated gastric and intestinal digestion. This conclusion was supported by correlation analysis between concentrations of free Fe(II) and As(III) (Fig. 2). Data showed that As(III) concentrations were significantly positively correlated with Fe(II) concentrations from goethite (R^2 = 0.919, p = 0.003) and hematite (R^2 = 0.965, p = 0.001) in simulated gastric fluid (Fig. 2a and 2b), analogous results were found in intestinal digestion (Fig. 2c and 2d). Time-dependent changes in dissolved Fe(II) and As(III) indicated that arsenite concentrations increased rapidly in gastric bio-fluid within the first 30 min, and then decreased to a slow but steady reduction rate in the rest of the digestive period (Fig. 2a and 2b). The gastric two-stage liberation phenomenon was attributed to different binding patterns between As and iron minerals. Most of arsenate reduced rapidly upon entry into the acidic gastric bio-fluid was likely initially adsorbed on goethite and hematite external surface. A lower amount of As was adsorbed on goethite and hematite internal surface as a result of intraparticle diffusions, leading to slow reduction rate. Comparatively, the aqueous As(III) concentrations in intestinal bio-fluid did not show an obvious two-stage phenomenon (Fig. 2c and 2d). This might be attributed to the interference from multiple digestive enzymes (bile salts and pancreatin) and inorganic ions (Fe^{2+} and HCO_3^-) on the mobilization and transformation of As.

3.4. Influence of digestive biochemistry on arsenic release

The preliminary experiment confirmed As release and reduction occurred in the simulated gastrointestinal bio-fluids. Based on the As bioaccessibility, we determined the influence of digestive enzymes and dietary components on As release and supplied a dietary strategy to alleviate the health risk of incidental As intake.

Facilitation of digestive enzymes on As release.—In the HCl addition system, As concentrations decreased with time, indicating that acid promoted aqueous As adsorption onto iron minerals in the absence of pepsin (Fig. 3a and 3b). Moreover, we observed a massive As release from As(V)-containing iron minerals in the presence of pepsin. The aqueous As concentrations were 1.66 and 2.07 mg/L for goethite and hematite in gastric digestion at 1 h, approximately 2 – 3 times of pepsin absence group. Pepsin enhanced As dissolution, leading to a significant increase of As bioaccessibility (Li et al., 2015).

Gastric chyme was subsequently digested in various intestinal components conditions to elucidate the roles of HCO_3^-, bile salts and pancreatin on As release. The amounts of As release followed the trend: binary components of bile salts and pancreatin group > single pancreatin group > single bile salts group > enzyme blank group (Fig. 3c and 3d). The results demonstrated the synergistic effect of HCO_3^-, bile salts and pancreatin on promoting As release. Arsenic concentrations in the enzymes blank group were 0.40 – 0.83 mg/L from goethite and 0.51 – 0.99 mg/L from hematite in intestinal digestion. HCO_3^- competed with arsenate for surface active sites of iron minerals and promoted As release, which was attributed to the similar tetrahedral anion structure of HCO_3^- and arsenate (Brechbühl et al., 2012). Arsenic concentrations in the single bile salts group were 0.73 – 0.86 mg/L from goethite and 0.99 – 1.08 mg/L from hematite. As for the single pancreatin group, As

concentrations were 0.72 – 0.99 mg/L from goethite and 1.01 – 1.41 mg/L from hematite in intestinal digestion. Organic components of bile salts and pancreatin enhanced As release by binding As to form metalloproteins, thus increasing As bioaccessibility in simulated gastrointestinal bio-fluids (Smith et al., 2014; Sharma et al., 2021).

Inhibition of calcium on As release.—We confirmed the significant ($p < 0.05$) efficacy of calcium ions as alleviator of As bioaccessibility in simulated gastrointestinal bio-fluids (Figure S3). The aqueous As concentrations decreased significantly at the two $CaCl_2$ concentration assayed (1 and 10 g/L). Under fasted states, As concentrations were 1.08 – 1.55 mg/L in gastric digestion at 1 h and 1.12 – 1.62 mg/L in intestinal digestion at 8 h, which decreased by up to 74.4% with 10 g/L $CaCl_2$ addition. The phenomenon of As release inhibition attributed to the formation of Ca-As complexes (Zhong et al., 2020). It indicated that calcium-rich food or drugs can be effective dietary supplement to alleviate As bioaccessibility in populations with high As exposure, such as dairy products, calcium tablet and bean products. In contrast, As bioaccessibility increased with the addition of sugar, starch, cellulose, glutathione and oleic acid (termed food matrix) in the simulated gastrointestinal bio-fluids. The maximum As concentration was 1.93 mg/L with glutathione addition. The major mechanisms of As release enhancement by the organic food matrix involved reductive dissolution, proton promotion, and ligand exchange for As-containing iron minerals dissolution (Bao et al., 2021). Besides, the food matrix was cleaved into smaller molecular fragments by digestive enzymes, these organic small molecules bound with iron minerals and participated in the formation of mineral microaggregates. The microaggregates occupied the adsorption sites and enhanced As release. Besides, organic ligands of food matrix have high affinities towards Fe(III) oxyhydroxides through complexation with structural Fe(III) and turning to soluble ligand-Fe(III) complexes, thus promoted As release. Taken together, the findings suggested that dietary habit greatly influenced the As bioaccessibility in the gastrointestinal tract, which should be incorporated into human health risk assessment of As-contaminated soil and dust.

3.5. Mineralogical analyses of solid-phase samples

Fourier Transform Infrared Spectroscopy of solid-phase samples.—Observation of ATR-FTIR confirmed the surface complexation between digestive enzymes and iron minerals, and the evolution of the functional groups on digestive enzymes during simulated gastrointestinal digestion (Figs. 4 and S4). The primary structures of pepsin and pancreatin are peptide and amino acid residues such as tryptophan and tyrosine, and the main functional groups include aromatic C, C=O and phenolic –OH (Xiao et al., 2020). The peaks between 1073 and 1163 cm^{-1} symbolized C—O (C—OH, C—O) groups and two peaks at 1519 and 1558 cm^{-1} were the stretching vibration of C=C group for digestive enzymes (Fig. 4a) (Fu et al., 2017; Zhang et al., 2022). The peaks of Fe—OH (~1067 cm^{-1}) disappeared and formed new C—O—C (C—OH, C—O) and C=C groups after gastrointestinal digestion, demonstrating the adsorption of enzymes on goethite surface (Song et al., 2015; Cheng et al., 2016). Similar results were found on hematite and goethite surface (Fig. 4b) (Fu et al., 2017; Zhang et al., 2022). The amino and carboxyl groups of proteases can be positively or negatively charge by proton association or dissociation, additionally, the hydroxyl groups of goethite and hematite have a variable surface charge. Therefore, we inferred that the amino

or carboxyl groups of proteases attached to the surface hydroxyl group on the hematite and goethite, thus leading to proteases adsorptive retention.

Wavenumbers of 1698 cm^{-1} (for goethite) and 1695 cm^{-1} (for hematite) were owing to the C=O group (Zhang et al., 2022). The peak intensity of OH group, locating at ~1655 cm^{-1} for goethite and ~1632 cm^{-1} for hematite, increased significantly after gastric digestion, while the peak of OH group disappeared and formed C=O bond after intestinal digestion. The electron-donating phenolic and electron-accepting quinone moieties were likely the dominant electron exchange moieties in dissolved organic matter (DOM) (Walpen et al., 2018). Thus, we inferred that phenolic –OH in pepsin and pancreatin was oxidized to the quinone through electron transfer to As(V) and Fe(III). Wavenumbers of 888 cm^{-1} and 791 cm^{-1} were attributed to the bending vibrations of δ-OH inward and γ-OH outward on the (001) plane of goethite (Xiao et al., 2020). The wavenumbers of 1488 and 1489 cm^{-1} were NO_3^-, and the bands at 1430 and 1394 cm^{-1} were attributed to CO_3^- (Zhang et al., 2020; Zhang et al., 2022). The As-O bond was not observed on As-containing goethite, which can be ascribed to the overlapping of the As-O bond and two OH bonds at 888 cm^{-1} and 791 cm^{-1} (Zhu et al., 2019). The peak at 801 cm^{-1} was attributed to As-O-Fe bidentate complexes for hematite (Brechbühl et al., 2012).

X-ray photoelectron spectroscopy of solid-phase samples.—XPS As3d spectra revealed that As(V) adsorbed on the iron minerals surface was reduced to As(III) after simulated gastrointestinal digestion. The characteristic peaks of As(V) and As(III) appeared at 45.1 eV and 44.8 eV for two As-containing iron minerals (Table S3) (Viltres et al., 2020). The goethite-sorbed As(V) was completely reduced to As(III) after gastric digestion for 1 h, while hematite-sorbed As(V) was not completely reduced to As(III) until intestinal digestion for 8 h (Fig 5a and 5b). This was attributable to complete reduction of As adsorbed on goethite surface but only partial reduction of As adsorbed on hematite in gastric bio-fluid. Goethite had a larger specific surface area and more active adsorption sites than hematite, which facilitated the contact of As and proteases, thus leading to the completely reduction of goethite-sorbed As and partially reduction of hematite-sorbed As (Yin et al., 2020; Yang et al., 2022). Moreover, all the As(III) resident on the hematite surface was released to gastric bio-fluid, thus leading to the peak of 100% As(V) on hematite after gastric digestion (Fig. 5a and 5b). Although goethite-sorbed As(V) had been completely reduced to As(III) after gastric bio-fluid digestion for 1 h, there was still As(V) release into intestinal bio-fluid. It was attributed to As(V) binding with oxygen-containing functional groups, such as carboxylic, amino, quinone and hydroxyl of proteinases, to form DOM-As complexes through ligand exchange (Biswas et al., 2019). Arsenate release from DOM-As complexes led to As increase in the intestinal bio-fluid.

The Fe2p spectra showed that 36.31% of Fe(III) was reduced to Fe(II) on residual goethite and hematite after 9 h of simulated gastrointestinal digestion (Table S3). Coordination between organic groups and –OH on the iron mineral surface was responsible for partial reduction of the Fe(III), as the iron atoms received electron clouds from oxygen atoms of pepsin group (Khaled, 2010). The binding energy at 724.0 and 718.0 eV corresponded to 2p1/2 orbit and satellite peak of the 2p3/2 orbit of Fe (Lu et al., 2014). The peaks at 710.7, 710.5 and 710.4 eV corresponded to Fe(II), and 712.9, 712.8 and 712.7 eV corresponded

to Fe(III) of goethite (Fig. 5c) (Liu et al., 2022). The peaks at 709.6, 710.2, and 710.3 eV attributed to Fe(II) of hematite, the peaks at 711.7, 712.2, and 712.3 eV attributed to Fe(III) (Fig. 5d) (Jung et al., 2014). The reductive dissolution of goethite and hematite in soils or dust played an important role in regulating As retention, and the increase in As bioaccessibility was associated with an increase in Fe solubilization and reduction (Yin et al., 2020).

The O1s spectra also confirmed the surface complexation between digestive enzymes and iron minerals, which was supported by new peaks corresponding to C—O bond at 532.2 and 532.4 eV after gastrointestinal digestion. The surface structural oxygen and hydroxyl groups of goethite were fitted into peaks at 529.5 – 529.7 eV and 530.7 – 530.9 eV, and for hematite, the peaks were corresponding to 529.0 – 529.2 eV and 530.5 – 530.7 eV (Jung et al., 2014). The percentage of surface structural oxygen decreased during 1 h of gastric digestion and then increased during 8 h of intestinal digestion (Fig. 5e). The phenomenon mainly attributed to the difference of pH between simulated gastric and intestinal bio-fluids. Part of the dissolved iron in gastric bio-fluid may be reprecipitated within the goethite during intestinal digestion at pH 6.5, thereby strengthening the peaks intensity of structural oxygen. There was no reprecipitation phenomenon for hematite during intestinal digestion (Fig. 5f). This can be explained by the differences that goethite had more adsorption sites for Fe(III) precipitates.

3.6. Proposed mechanism of arsenic release in simulated bio-fluid

Gastric phase.—As-containing iron minerals interacted with acid and pepsin when they were ingested and exposed to simulated gastric bio-fluid (Fig. 6a). Acid dissolution of iron minerals led to the release of As(V) and Fe(III) in gastric bio-fluid. Besides, organic ligands of pepsin were adsorbed onto the iron minerals surface, they not only competed with As, but also caused the slow dissolution of iron minerals and As release. Subsequently, the released As(V) and Fe(III) were reduced to As (III) and Fe(II) by aqueous pepsin (Eq. (1) and Eq. (2)). Additionally, pepsin also reduce As(V) to As(III) directly on goethite and hematite surface, where after, As(III) was partially released to gastric biofluid and partially retained on iron minerals surface (Eq. (3)). The point of zero charges of pepsin ($PZC_{pepsin.}$) was 1.0 and pepsin surface developed negative charge at gastric pH > $PZC_{pepsin.}$ by proton dissociation (Peng et al., 2019).

Intestinal phase.—Following the gastric digestion, As-containing iron minerals continued dissolution and As released in the simulated intestinal bio-fluid, which was synergistically promoted by $NaHCO_3$, bile salt and pancreatin (Fig. 6b). The added HCO_3^- competed with arsenate for surface adsorption sites of iron minerals and facilitated As release. Bile salt and pancreatin have high complexation capacity to compete with iron minerals for As complexing, accelerating As release in intestinal bio-fluid. The released As(V) was reduced to As(III) by pancreatin and freshly generated Fe(II) in gastric digests (Eq. (4) and Eq. (5)). Besides, pancreatin acted as the dominant electron donor in intestinal bio-fluid, also reduced Fe(III) in aqueous phase as well as As(V) and Fe(III) in solid phase (Eq. (6) and Eq. (7)). Correspondingly, phenolic-OH of pepsin and pancreatin was oxidized to quinone. The $PZC_{pancreatin}$ was 10.5 and pancreatin surface developed positive charge at intestinal

pH < $PZC_{pancreatin}$. by proton association (Peng et al., 2019). These results revealed the role of multiple digestive enzymes for As mobilization and transformation in simulated gastrointestinal bio-fluids.

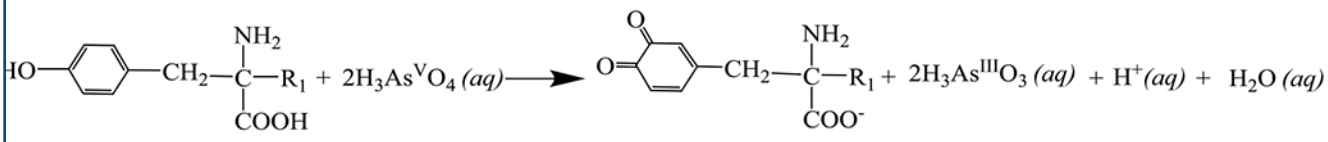

(1)

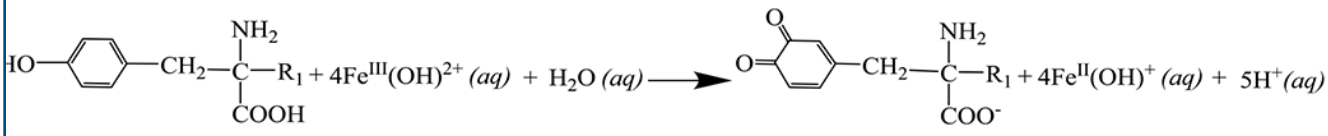

(2)

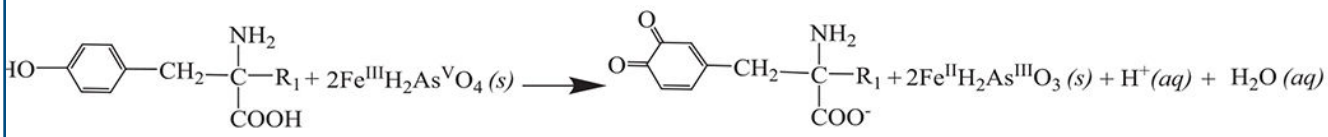

(3)

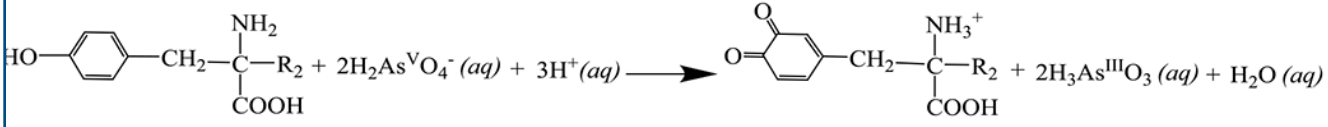

(4)

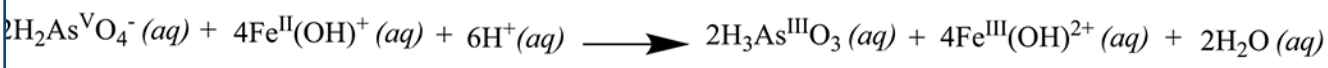

(5)

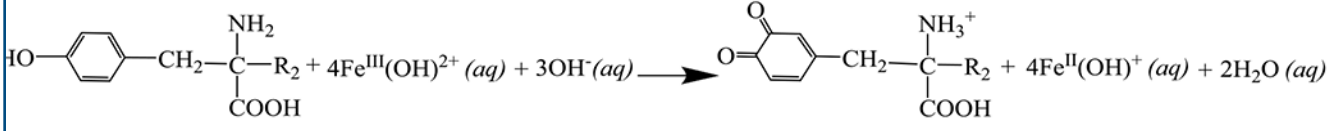

(6)

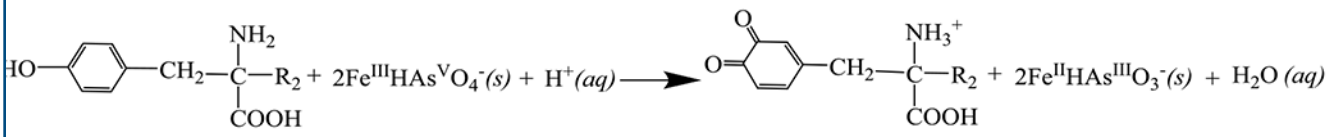

(7)

4. Conclusions

The iron (hydr)oxides-sorbed As(V) released and simultaneously transformed to highly toxic As(III) during simulated gastrointestinal digestion. Due to the different crystalline structure and As-Fe complexation modes, the potential exposure risk of As-containing hematite was higher than goethite. The reaction mechanisms of As associated with iron (hydr)oxides in simulated gastrointestinal bio-fluids were previously ignored. This work proved that As release and reduction was mainly coupled with acid dissolution and reductive dissolution of iron minerals. Besides, pepsin and pancreatin enhanced As release from As-containing iron minerals, acting as electron donor for As(V) reduction to As(III). Iron (hydr)oxides also acted as an electron acceptor and had a unique contribution to As mobilization and transformation. Proteases caused the reductive dissolution of As(V)-bearing Fe(III)-(oxyhydr)oxides and the reduction of solid-phase As(V), releasing As(III) to the aqueous phase. Correspondingly, phenolic –OH in pepsin and pancreatin was oxidized to the quinone. It deepened our understanding of Fe minerals and digestive enzymes in human health risk assessment associated with soil and dust As exposures. In addition, calcium-rich food or drugs may be effective dietary supplement to alleviate the As bioaccessibility in simulated gastrointestinal tract. The results have important environmental health implications for modulating As bioaccessibility and alleviating the adverse impact of As exposure via accidental soil and dust ingestion. It should be noted that conclusions from the *in vitro* assay are indicative, and further comprehensive studies including practical soil or dust samples and *in vivo* validation is required for confirmation of *in vivo-in vitro* predictive relationships.

Supplementary Material

Refer to Web version on PubMed Central for supplementary material.

Acknowledgements

The work was financially supported by the National Natural Science Foundation of China (No. 42272309), the National Institute of Environmental Health Sciences (NIEHS) Superfund Research Program Grant P42 ES04940, the Open Project of Technology Innovation Center for Ecological Evaluation and Remediation of Agricultural Land in Plain Area, Ministry of Natural Resources (No. ZJGCJ202003) and the special fund from the Hubei Provincial Engineering Research Center of Systematic Water Pollution Control (China University of Geosciences, Wuhan, P. R. China) (No. G1323519366).

Data availability

Data will be made available on request.

References

Bao Y, Bolan NS, Lai J, Wang Y, Jin X, Kirkham MB, Wu X, Fang Z, Zhang Y, Wang H, 2021. Interactions between organic matter and Fe (hydr)oxides and their influences on immobilization and remobilization of metal(loid)s: a review. Crit. Rev. Environ. Sci. Technol 52 (22), 4016–4037.

Barron A, Sun J, Passaretti S, Sbarbati C, Barbieri M, Colombani N, Jamieson J, Bostick BC, Zheng Y, Mastrocicco M, Petitta M, Prommer H, 2022. In situ arsenic immobilisation for coastal aquifers using stimulated iron cycling: lab-based viability assessment. Appl. Geochem 136, 105155. [PubMed: 34955596]

Biswas A, Besold J, Sjöstedt C, Gustafsson JP, Scheinost AC, Planer-Friedrich B, 2019. Complexation of arsenite, arsenate, and monothioarsenate with oxygen-containing functional groups of natural organic matter: an XAS study. Environ. Sci. Tech 53 (18), 10723–10731.

Brechbühl Y, Christl I, Elzinga EJ, Kretzschmar R, 2012. Competitive sorption of carbonate and arsenic to hematite: combined ATR-FTIR and batch experiments. J. Colloid Interface Sci 377 (1), 313–321. [PubMed: 22494686]

Cai X, Wang P, Li Z, Li Y, Yin N, Du H, Cui Y, 2020a. Mobilization and transformation of arsenic from ternary complex OM-Fe(III)-As(V) in the presence of As(V)-reducing bacteria. J. Hazard. Mater 381, 120975. [PubMed: 31445471]

Cai X, ThomasArrigo LK, Fang X.u., Bouchet S, Cui Y, Kretzschmar R, 2020b. Impact of organic matter on microbially-mediated reduction and mobilization of arsenic and iron in arsenic(V)-bearing ferrihydrite. Environ. Sci. Tech 55 (2), 1319–1328.

Cheng Z, Fu F, Dionysiou DD, Tang B, 2016. Adsorption, oxidation, and reduction behavior of arsenic in the removal of aqueous As(III) by mesoporous Fe/Al bimetallic particles. Water Res. 96, 22–31. [PubMed: 27016635]

Clemente MJ, Devesa V, Vélez D, 2016. Dietary strategies to reduce the bioaccessibility of arsenic from food matrices. J. Agric. Food Chem 64 (4), 923–931. 10.1021/acs.jafc.5b04741. [PubMed: 26766512]

Dixit S, Hering JG, 2003. Comparison of arsenic(V) and arsenic(III) sorption onto iron oxide minerals: implications for arsenic mobility. Environ. Sci. Tech 37 (18), 4182–4189. 10.1021/es030309t.

Fu D, He Z, Su S, Xu B, Liu Y, Zhao Y, 2017. Fabrication of α-FeOOH decorated graphene oxide-carbon nanotubes aerogel and its application in adsorption of arsenic species. J. Colloid Interface Sci 505, 105–114. [PubMed: 28577460]

Guerra A, Etienne-Mesmin L, Livrelli V, Denis S, Blanquet-Diot S, Alric M, 2012. Relevance and challenges in modeling human gastric and small intestinal digestion. Trends Biotechnol. 30 (11), 591–600. [PubMed: 22974839]

Hammond CM, Root RA, Maier RM, Chorover J, 2020. Arsenic and iron speciation and mobilization during phytostabilization of pyritic mine tailings. Geochim. Cosmochim. Acta 286, 306–323. [PubMed: 33071297]

Hong J, Liu L, Luo Y, Tan W, Qiu G, Liu F, 2018. Photochemical oxidation and dissolution of arsenopyrite in acidic solutions. Geochim. Cosmochim. Acta 239, 173–185.

Juhasz AL, Smith E, Nelson C, Thomas DJ, Bradham K, 2014. Variability associated with As *in vivo-in vitro* correlations when using different bioaccessibility methodologies. Environ. Sci. Tech 48 (19), 11646–11653.

Jung S, Bae S, Lee W, 2014. Development of Pd-Cu/hematite catalyst for selective nitrate reduction. Environ. Sci. Tech 48 (16), 9651–9658. 10.1021/es502263p.

Khaled KF, 2010. Studies of iron corrosion inhibition using chemical, electrochemical and computer simulation techniques. Electrochim. Acta 55 (22), 6523–6532. 10.1016/j.electacta.2010.06.027.

Li M-Y, Chen X-Q, Wang J-Y, Wang H-T, Xue X-M, Ding J, Juhasz AL, Zhu Y-G, Li H-B, Ma LQ, 2021. Antibiotic exposure decreases soil arsenic oral bioavailability in mice by disrupting ileal microbiota and metabolic profile. Environ. Int 151, 106444. [PubMed: 33621917]

Li H-B, Li J, Zhu Y-G, Juhasz AL, Ma LQ, 2015. Comparison of arsenic bioaccessibility in housedust and contaminated soils based on four *in vitro* assays. Sci. Total Environ 532, 803–811. [PubMed: 26136157]

Lin C, Wang B, Cui X, Xu D, Cheng H, Wang Q, Ma J, Chai T, Duan X, Liu X, Ma J, Zhang X, Liu Y, 2017. Estimates of soil ingestion in a population of Chinese children. Environ. Health Perspective 125 (7), 077002.

Liu K, Li F, Pang Y, Fang L, Hocking R, 2022. Electron shuttle-induced oxidative transformation of arsenite on the surface of goethite and underlying mechanisms. J. Hazard. Mater 425, 127780. [PubMed: 34801297]

Lu X, Zeng Y, Yu M, Zhai T, Liang C, Xie S, Balogun M-S, Tong Y, 2014. Oxygen-deficient hematite nanorods as high-performance and novel negative electrodes for flexible asymmetric supercapacitors. Adv. Mater 26 (19), 3148–3155. [PubMed: 24496961]

Menacherry SPM, Kim K, Lee W, Choi CH, Choi W, 2018. Ligand-specific dissolution of iron oxides in frozen solutions. Environ. Sci. Tech 52 (23), 13766–13773.

Meunier L, Walker SR, Wragg J, Parsons MB, Koch I, Jamieson HE, Reimer KJ, 2010. Effects of soil composition and mineralogy on the bioaccessibility of arsenic from tailings and soil in gold mine districts of Nova Scotia. Environ. Sci. Tech 44 (7), 2667–2674.

Notini L, Latta DE, Neumann A, Pearce CI, Sassi M, N'Diaye AT, Rosso KM, Scherer MM, 2018. The role of defects in Fe(II)-goethite electron transfer. Environ. Sci. Tech 52 (5), 2751–2759.

Peng Q, Liu J, Zhang T, Zhang T-X, Zhang C-L, Mu H, 2019. Digestive enzyme corona formed in the gastrointestinal tract and its impact on epithelial cell uptake of nanoparticles. Biomacromolecules 20 (4), 1789–1797. [PubMed: 30893550]

Rahaman MS, Rahman MM, Mise N, Sikder MT, Ichihara G, Uddin MK, Kurasaki M, Ichihara S, 2021. Environmental arsenic exposure and its contribution to human diseases, toxicity mechanism and management. Environ. Pollut 289, 117940. [PubMed: 34426183]

Schwertmann U, Cornell RM, 2000. Iron oxides in the laboratory: preparation and characterization. 2nd, ed.; Wiley VCH: Weinheim, Germany. 67–134.

Sharma P, Pandey AK, Udayan A, et al. , 2021. Role of microbial community and metal-binding proteins in phytoremediation of heavy metals from industrial wastewater. Bioresour. Technol 326 (124750), 1–10. 10.1016/j.biortech.2021.124750.

Smith E, Scheckel K, Miller BW, Weber J, Juhasz AL, 2014. Influence of *in vitro* assay pH and extractant composition on As bioaccessibility in contaminated soils. Sci. Total Environ 473-474, 171–177. [PubMed: 24369295]

Song J, Jia S-Y, Yu B.o., Wu S-H, Han X.u., 2015. Formation of iron (hydr)oxides during the abiotic oxidation of Fe(II) in the presence of arsenate. J. Hazard. Mater 294, 70–79. [PubMed: 25855615]

Thomas AN, Root RA, Lantz RC, Sáez AE, Chorover J, 2018. Oxidative weathering decreases bioaccessibility of toxic metal(loid)s in PM_{10} emissions from sulfide mine tailings. GeoHealth. 2 (4), 118–138. [PubMed: 30338309]

Tian X, Yu XH, 2013. The demand for nutrients in China. Front. Econ. China 8 (2), 186–206. 10.3868/s060-002-013-0009-9.

Van de Wiele T, Gallawa CM, Kubachk KM, Creed JT, Basta N, Dayton EA, Whitacre S, Laing GD, Bradham K, 2010. Arsenic metabolism by human gut microbiota upon *in vitro* digestion of contaminated soils. Environ. Health Perspect 118 (7), 1004–1009. [PubMed: 20603239]

Viltres H, Odio OF, Lartundo-Rojas L, et al. , 2020. Degradation study of arsenic oxides under XPS measurements. Appl. Surf. Sci 511 (145606), 1–10. 10.1016/j.apsusc.2020.145606.

Walpen N, Getzinger GJ, Schroth MH, Sander M, 2018. Electron-donating phenolic and electron-accepting quinone moieties in peat dissolved organic matter: quantities and redox transformations in the context of peat biogeochemistry. Environ. Sci. Tech 52 (9), 5236–5245.

Wan X, Xiang W.u., Wan N, Yan S, Bao Z, Wang Y, 2018. Complexation and reduction of iron by phenolic substances: implications for transport of dissolved Fe from peatlands to aquatic ecosystems and global iron cycling. Chem. Geol 498, 128–138.

Wang PC, Xue JH, Zhu ZM, 2021. Comparison of heavy metal bioaccessibility between street dust and beach sediment: particle size effect and environmental magnetism response. Sci. Total Environ 777 (146081), 1–9. 10.1016/j.scitotenv.2021.146081.

Wang P, Yin N, Cai X, Du H, Li Z, Sun G, Cui Y, 2018. Nutritional status affects the bioaccessibility and speciation of arsenic from soils in a simulator of the human intestinal microbial ecosystem. Sci. Total Environ 644, 815–821. [PubMed: 29990930]

Xiao Q.i., Liang J, Luo H, Li H, Yang J, Huang S, 2020. Investigations of conformational structures and activities of trypsin and pepsin affected by food colourant allura red. J. Mol. Liq 319, 114359.

Xiao Z, Xie X, Pi K, Gong J, Wang Y, 2021. Impact of organic matter on arsenic mobilization induced by irrigation in the unsaturated and saturated zones. J. Hydrol 602, 126821.

Yan Y, Wan B, Mansor M, Wang X, Zhang Q, Kappler A, Feng X, 2022. Co-sorption of metal ions and inorganic anions/organic ligands on environmental minerals: A review. Sci. Total Environ 803, 149918. [PubMed: 34482133]

Yang Z, Zhang N, Sun B, Su S, Wang Y, Zhang Y, Wu C, Zeng X, 2022. Contradictory tendency of As(V) releasing from Fe-As complexes: influence of organic and inorganic anions. Chemosphere 286, 131469. [PubMed: 34340118]

Yin N, Cai X, Zheng L, Du H, Wang P, Sun G, Cui Y, 2020. *In vitro* assessment of arsenic release and transformation from As(V)-sorbed goethite and jarosite: the influence of human gut microbiota. Environ. Sci. Tech 54 (7), 4432–4442.

Yin N, Li Y, Cai X, Du H, Wang P, Han Z, Sun G, Cui Y, 2021. The role of soil arsenic fractionation in the bioaccessibility, transformation, and fate of arsenic in the presence of human gut microbiota. J. Hazard. Mater 401, 123366. [PubMed: 32659581]

Yin N, Cai X, Wang P, Feng R, Du H, Fu Y, Sun G, Cui Y, 2022. Predictive capabilities of *in vitro* colon bioaccessibility for estimating *in vivo* relative bioavailability of arsenic from contaminated soils: arsenic speciation and gut microbiota considerations. Sci. Total Environ 818, 151804. [PubMed: 34808186]

Yu H, Wu B, Zhang X-X, Liu S.u., Yu J, Cheng S, Ren H-Q, Ye L, 2016. Arsenic metabolism and toxicity influenced by ferric iron in simulated gastrointestinal tract and the roles of gut microbiota. Environ. Sci. Tech 50 (13), 7189–7197.

Zhang Y, Cao J, Wang X, Liu H, Shao Y.i., Chu C, Xue F, Bai J, 2022. The effect of enzymes on the *in vitro* degradation behavior of Mg alloy wires in simulated gastric fluid and intestinal fluid. Bioact. Mater 7, 217–226. [PubMed: 34466728]

Zhang X, Zhang L, Liu Y, Li M.i., Wu X, Jiang T, Chen C, Peng Y, 2020. Mn-substituted goethite for uranium immobilization: a study of adsorption behavior and mechanisms. Environ. Pollut 262, 114184. [PubMed: 32193078]

Zhong D, Zhao Z, Jiang Y.i., Yang X, Wang L, Chen J, Guan C-Y, Zhang Y, Tsang DCW, Crittenden JC, 2020. Contrasting abiotic As (III) immobilization by undissolved and dissolved fractions of biochar in Ca^{2+}-rich groundwater under anoxic conditions. Water Res. 183, 116106. [PubMed: 32771717]

Zhu M, Hu X, Tu C, Zhang H, Song F, Luo Y, Christie P, 2019. Sorption mechanisms of diphenylarsinic acid on ferrihydrite, goethite and hematite using sequential extraction, FTIR measurement and XAFS spectroscopy. Sci. Total Environ 669, 991–1000. [PubMed: 30970466]

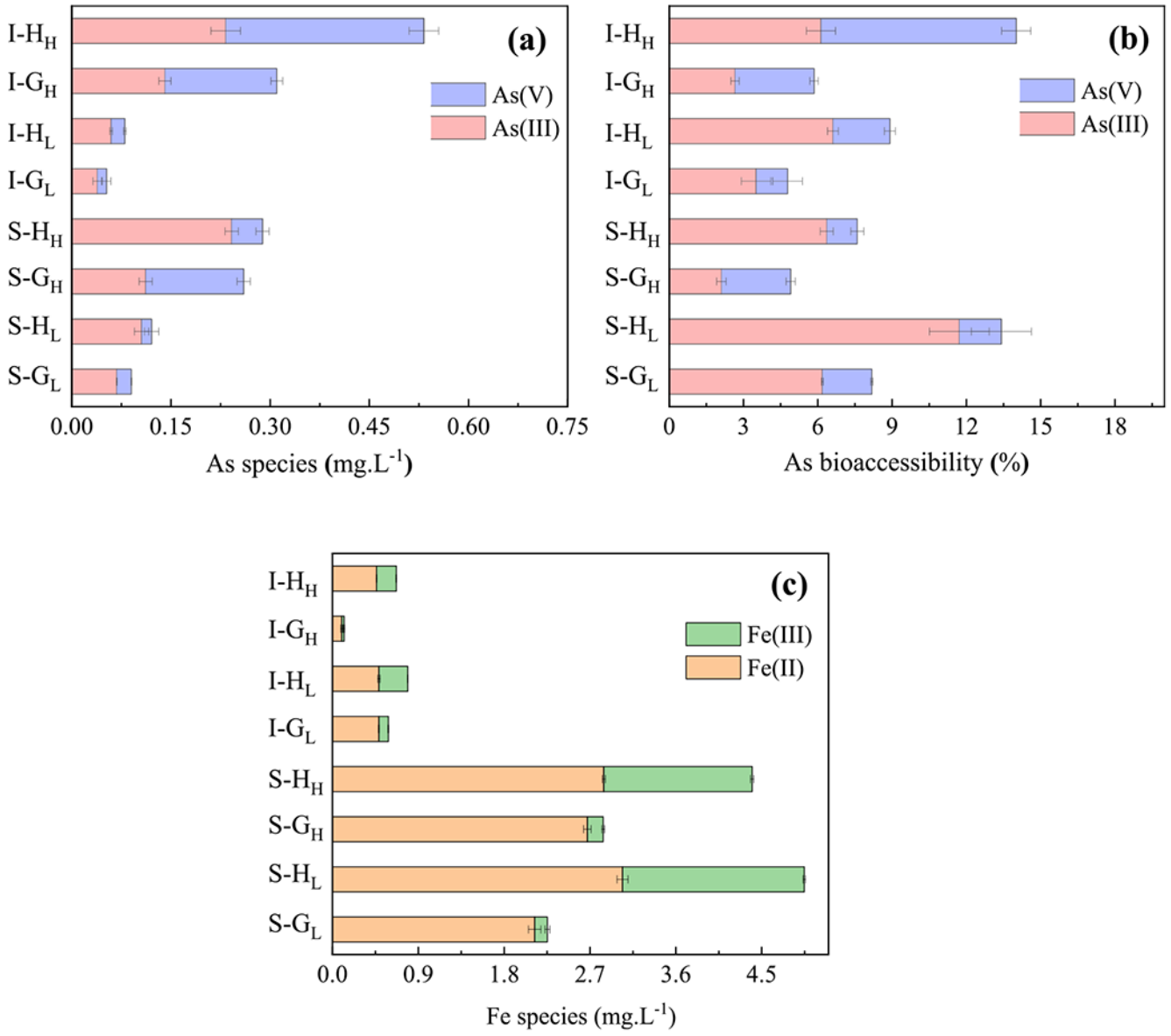

Fig. 1.

(a) Concentrations and (b) bioaccessibility of dissolved As species, (c) concentrations of dissolved Fe species in simulated gastrointestinal bio-fluid. S-H_H and I-G_L, represented high and low As adsorption on hematite (H) and goethite (G) in simulated gastric (S) and intestinal (I) bio-fluids. Gastric conditions: 1% pepsin, pH 1.5 ± 0.1, 37°C, 200 rpm, anaerobic. Intestinal conditions: 3.6 g/L bile salt, 0.36 g/L pancreatin, pH 6.5 ± 0.1, 37°C, 200 rpm, anaerobic. Values are mean error bars ± SD in triplicate.

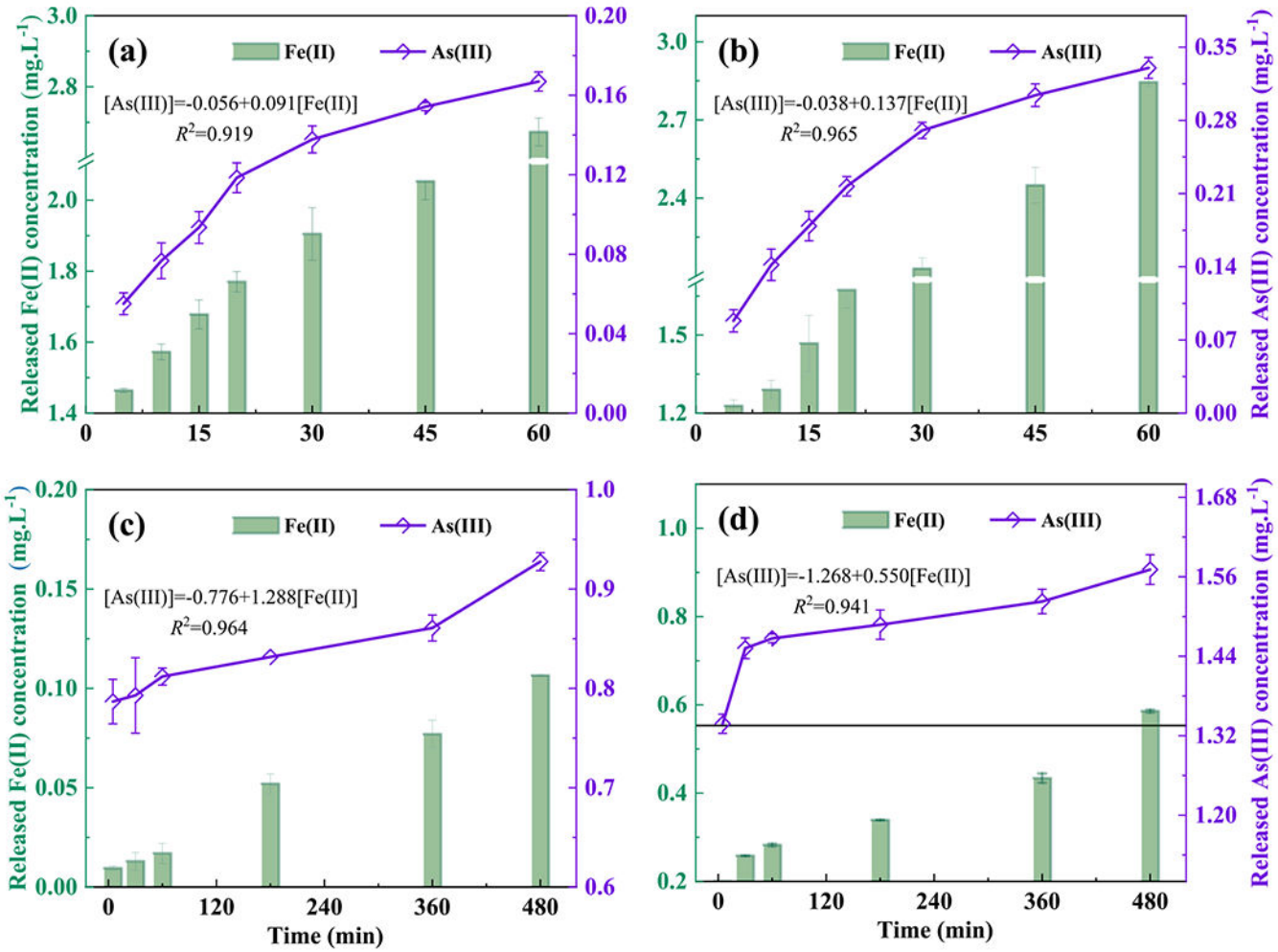

Fig. 2.

Concentrations of dissolved As(III) (line) and Fe(II) (bar) with time for (a) G_H in simulated gastric bio-fluid, (b) H_H in simulated gastric bio-fluid, (c) G_H in simulated intestinal bio-fluid and (d) H_H in simulated intestinal bio-fluid. Gastrointestinal conditions were consistent with Fig. 1. Values are mean error bars ± SD in triplicate. Note axis break in (a) and (b).

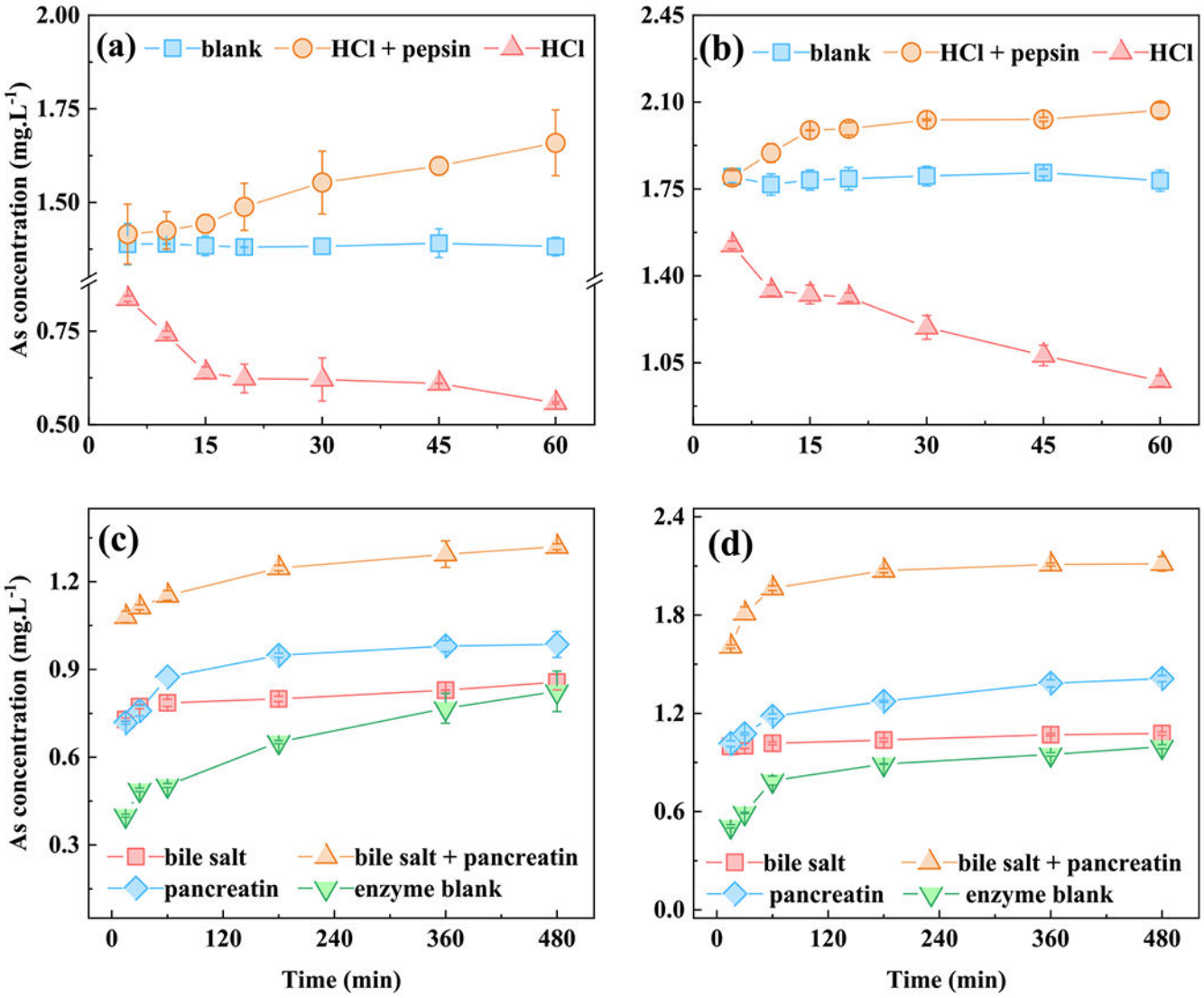

Fig. 3.

Dissolved As concentrations with time. (a) G_H in simulated gastric bio-fluid, (b) H_H in simulated gastric bio-fluid, (c) G_H in simulated intestinal bio-fluid and (d) H_H in simulated intestinal bio-fluid. Gastric conditions for (a) and (b): with/without 1 % pepsin, pH 1.5 ± 0.1, 37°C, 200 rpm, anaerobic. Intestinal conditions for (c) and (d): with/without 3.6 g/L bile salt and/or 0.36 g/L pancreatin, pH 6.5 ± 0.1, 37°C, 200 rpm, anaerobic. Values are mean error bars ± SD in triplicate. Note axis break in (a).

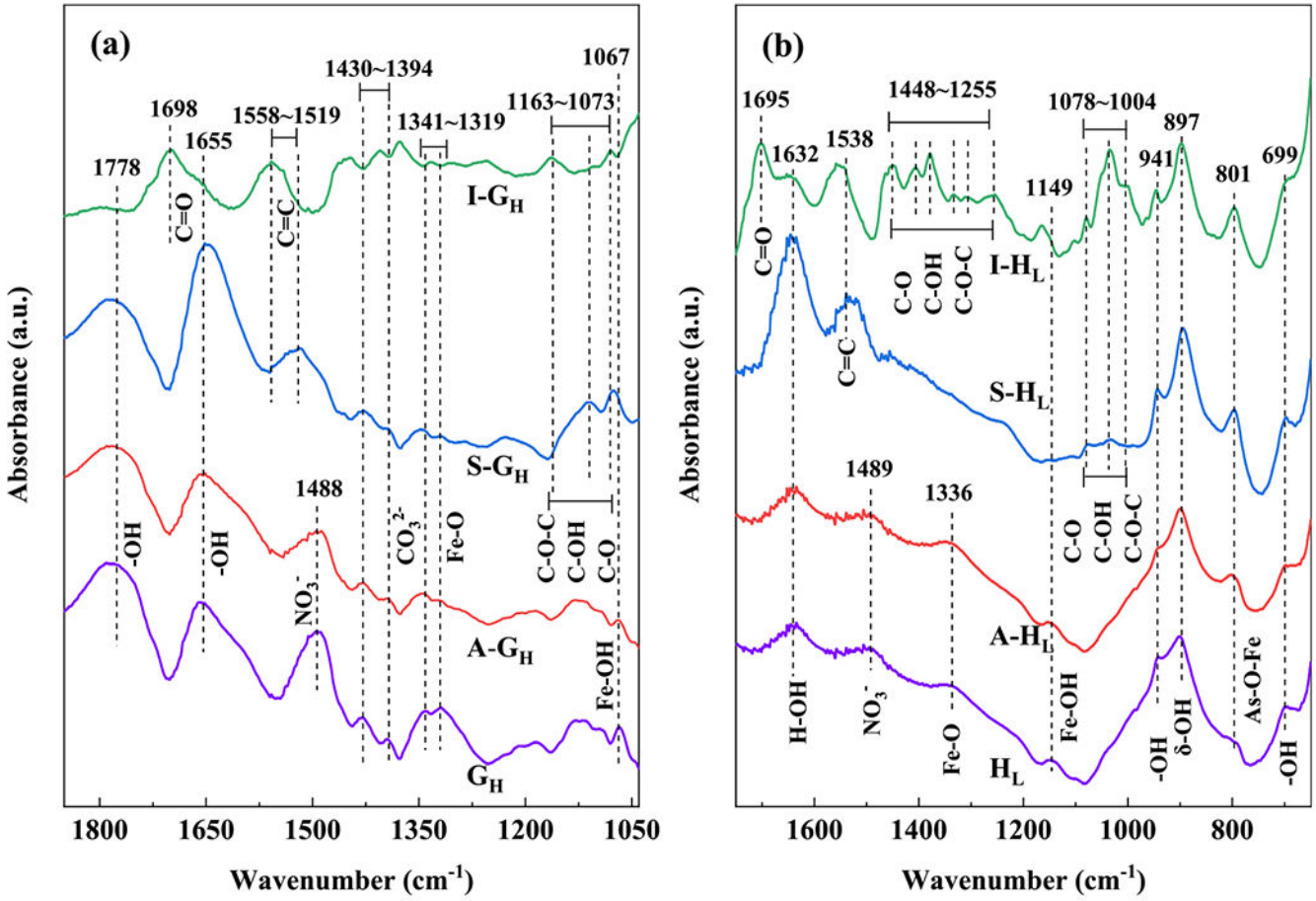

Fig. 4.

ATR-FTIR spectra of (a) goethite and (b) hematite. Line G_H and line H_H represented original goethite and hematite, line A-G_H and line A-H_H represented As-containing goethite and hematite, line S-G_H and line S-H_H were after gastric digestion, line I-G_H and line I-H_H were after intestinal digestion. Gastrointestinal conditions were consistent with Fig. 1.

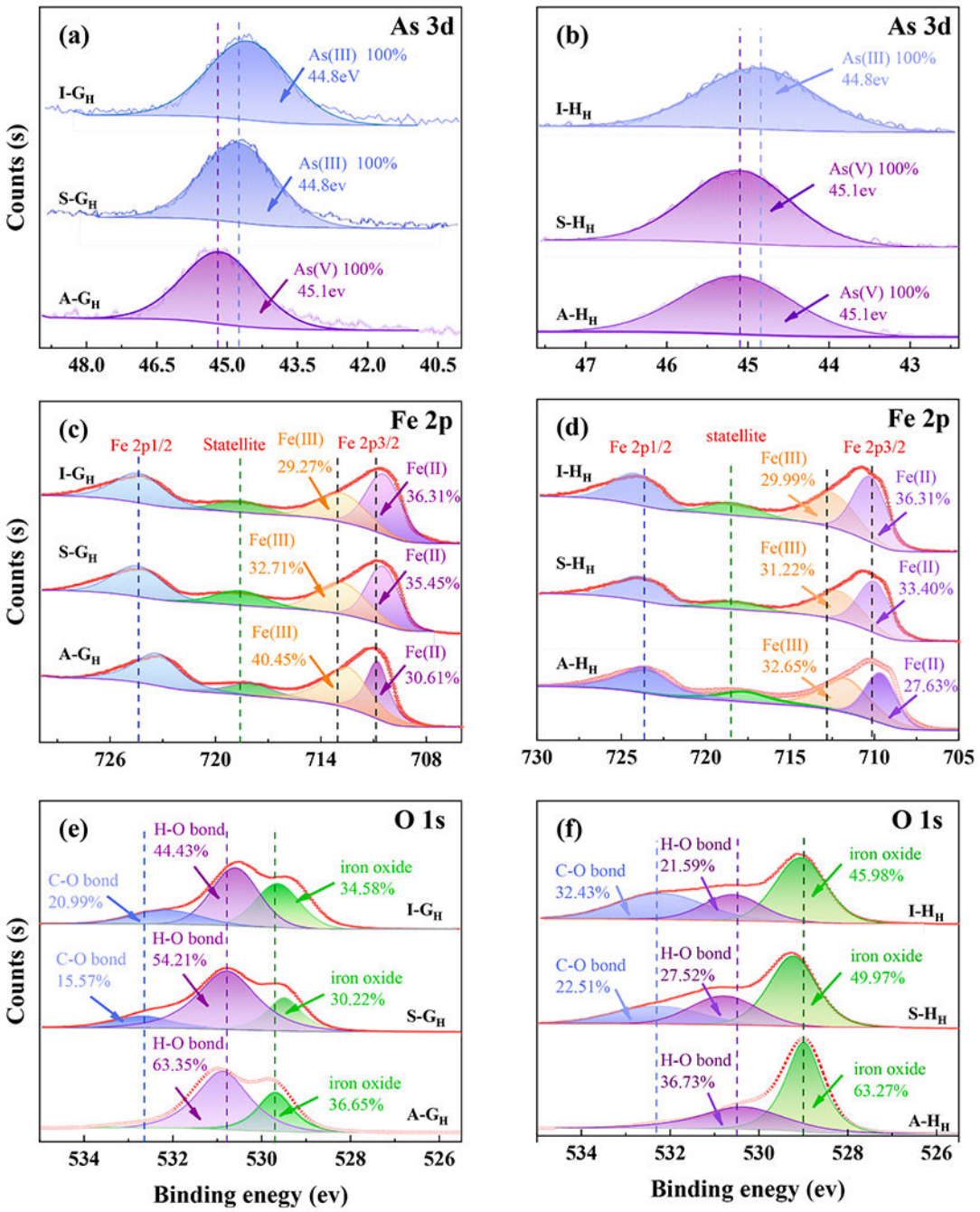

Fig. 5.

XPS As3d spectra of (a) goethite and (b) hematite; Fe2p spectra of (c) goethite and (d) hematite; O1s spectra of (e) goethite and (f) hematite. Line A-G_H and line A-H_H represented As-containing goethite and hematite, line S-G_H and line S-H_H were after simulated gastric digestion, line I-G_H and line I-H_H were after simulated intestinal digestion. Gastrointestinal conditions were consistent with Fig. 1. Peak parameter details are given in the SI (Table S3).

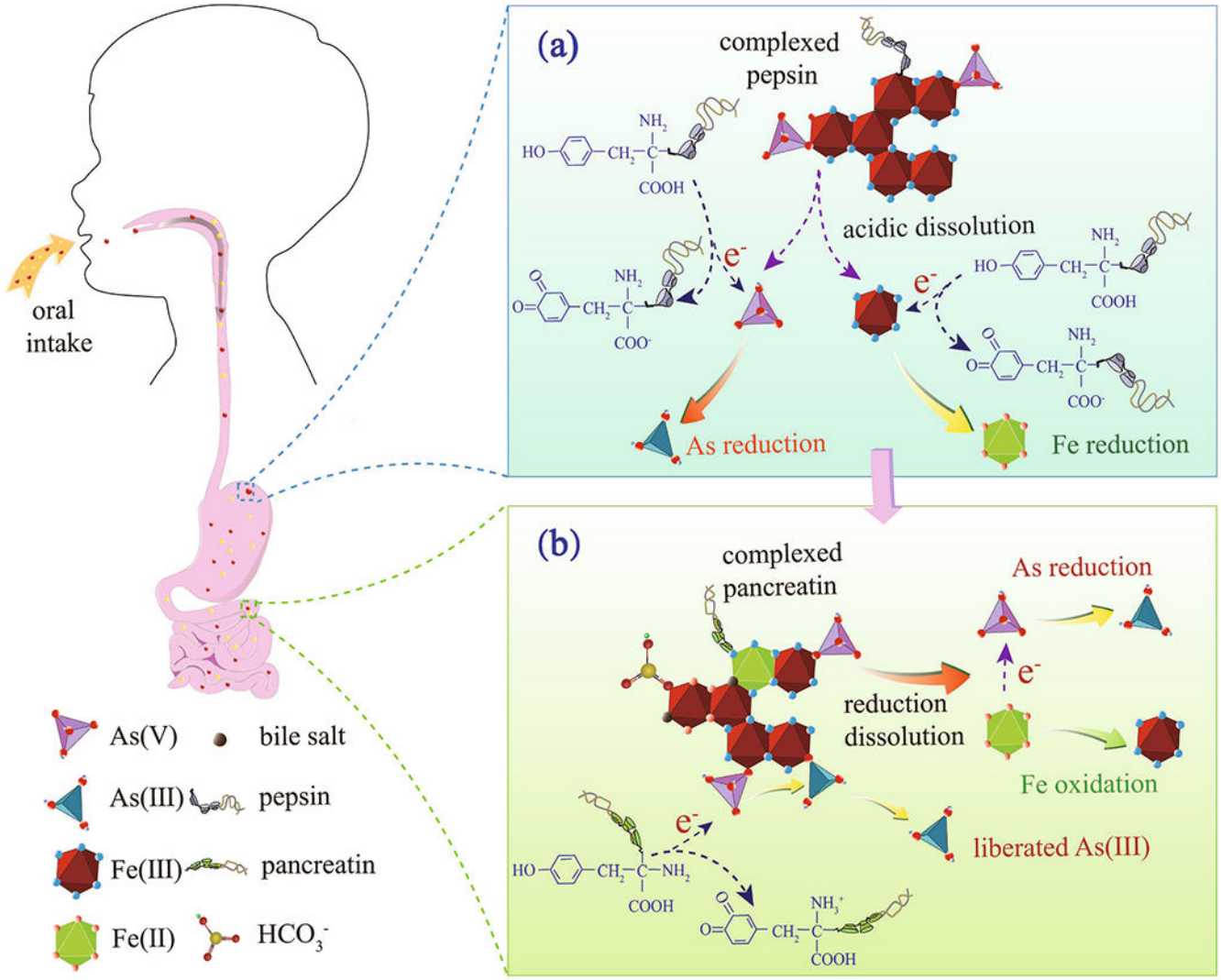

Fig. 6.

Schematic illustration of the possible transformation mechanism toward iron minerals-sorbed As in (a) simulated gastric and (b) intestinal bio-fluids. Take the tyrosine in the structure of proteinases as an example.

Table 1

Total As and Fe release in the simulated gastric and intestinal bio-fluids of As(V)-containing iron minerals.[a]

Samples	As release amount /(mg.L^{-1}	As release rate/(ug.L^{-1}.min^{-1})	As bioaccessibility/(%)	Fe release amount/(mg.L^{-1}	Fe release rate/(μg.L^{-1}.min^{-1})	Fe bioaccessibility/(%)
S-G_L	0.090 ± 0.003	1.50 ± 0.05	8.18 ± 0.27	2.25 ± 0.06	40.83 ± 1.00	0.245 ± 0.006
S-H_L	0.120 ± 0.006	2.00 ± 0.10	13.33 ± 0.67	4.95 ± 0.04	82.50 ± 0.67	0.495 ± 0.004
S-G_H	0.26 ± 0.02	4.30 ± 0.30	4.91 ± 0.38	2.84 ± 0.02	47.33 ± 0.33	0.284 ± 0.002
S-H_H	0.29 ± 0.03	4.80 ± 0.50	7.63 ± 0.79	4.40 ± 0.03	73.33 ± 0.50	0.440 ± 0.003
I-G_L	0.052 ± 0.003	0.108 ± 0.006	4.73 ± 0.27	0.59 ± 0.02	1.23 ± 0.33	0.059 ± 0.002
I-H_L	0.070 ± 0.001	0.146 ± 0.002	7.78 ± 0.11	0.79 ± 0.03	1.65 ± 0.50	0.079 ± 0.003
I-G_H	0.31 ± 0.01	0.65 ± 0.02	5.85 ± 0.19	0.13 ± 0.01	0.27 ± 0.17	0.013 ± 0.001
I-H_H	0.53 ± 0.01	1.10 ± 0.02	13.95 ± 0.26	0.67 ± 0.01	1.40 ± 0.17	0.067 ± 0.001

[a] S-H_H and I-G_L, represented high and low As adsorption on hematite (H) and goethite (G) in the simulated gastric (S) and intestinal (I) bio-fluids. Values are mean ± SD in triplicate. Gastric conditions: 1 % pepsin, pH 1.5 ± 0.1, 37°C, 200 rpm, reaction time 1 h, anaerobic. Intestinal conditions: 3.6 g/L bile salt, 0.36 g/L pancreatin, pH 6.5 ± 0.1, 37°C, 200 rpm, reaction time 8 h, anaerobic. The As bioaccessibility was calculated as a ratio of As release amount from As-containing iron minerals relative to the total As concentration in As-containing iron minerals. The total As concentration in G_H and G_L was 5.3 and 1.1 mg/g, and for H_H and H_L, the values are 3.8 and 0.9 mg/g. Similarly, the Fe bioaccessibility was calculated as a ratio of Fe release amount from As-containing iron minerals relative to the total Fe mass of As-containing iron minerals. The total Fe mass of goethite and hematite were 0.01g.

Table 2

The effects of pepsin, bile salt and pancreatin on the release and speciation of As and Fe.[a]

Sample	Experimental condition	Total As/(mg.L^{-1})	As(III)/(mg.L^{-1})	Total Fe/(mg.L^{-1})	Fe(II)/(mg.L^{-1}
S-G_H	pepsin	0.26 ± 0.05	0.11 ± 0.01	2.84 ± 0.02	2.67 ± 0.04
	no pepsin	0.120 ± 0.002	ND	2.86 ± 0.02	ND
S-H_H	pepsin	0.29 ± 0.01	0.24 ± 0.01	4.40 ± 0.03	2.85 ± 0.02
	no pepsin	0.13 ± 0.01	ND	4.29 ± 0.03	ND
	bile	0.030 ± 0.003	ND	ND	ND
I-G_H	pancreatin	0.250 ± 0.005	0.090 ± 0.001	ND	ND
	bile + pancreatin	0.300 ± 0.007	0.120 ± 0.005	ND	ND
	bile	0.040 ± 0.003	ND	0.56 ± 0.01	0.44 ± 0.02
I-H_H	pancreatin	0.40 ± 0.01	0.050 ± 0.001	ND	ND
	bile + pancreatin	0.27 ± 0.06	0.140 ± 0.001	0.22 ± 0.01	0.16 ± 0.01

[a] S-H_H and I-G_H, represented high As adsorption on hematite (H) and goethite (G) in the simulated gastric (S) and intestinal (I) bio-fluids. Gastric conditions for S-G_H and S-H_H: with/without 1 % pepsin, pH 1.5 ± 0.1, 37°C, 200 rpm, reaction time 1 h, anaerobic. The results for I-G_H and I-H_H came from intestinal phase without gastric digests. NG-intestinal conditions: with/without 3.6 g/L bile salt and/or 0.36 g/L pancreatin, pH 6.5 ± 0.1, 37°C, reaction time 8 h, anaerobic. Values are mean ± SD in triplicate. ND represented not detected.